Surface electronic structure of epitaxial Ce and La films

E. Weschke, A. Höhr, and G. Kaindl
Institut für Experimentalphysik, Freie Universität Berlin, Arnimallee 14, D-14195 Berlin-Dahlem, Germany

S. L. Molodtsov,* S. Danzenbächer, M. Richter,† and C. Laubschat
Institut für Oberflächen- und Mikrostrukturphysik, Technische Universität Dresden, D-01062 Dresden, Germany

(Received 10 March 1998)

We report on a detailed photoemission (PE) study of monocrystalline Ce and La metal films grown on W(110). Angle-resolved PE reveals that both systems have very similar valence-band structures, with the observed dispersions being in good agreement with local-density approximation band-structure calculations. These calculations were performed for three different close-packed crystal structures of La and Ce metal, giving evidence for a double hcp structure of the films, i.e., a β phase in the case of Ce. The pronounced surface state, characteristic for the close-packed surfaces of trivalent lanthanide metals, is shown to exist also for β-Ce(0001), extending over a wide range of the surface Brillouin zone. The $4f$ electronic structure of the Ce film was studied by resonant PE at the $4d \rightarrow 4f$ threshold. A separation of bulk and surface contributions with high resolution was achieved by quenching the surface signal with a Dy overlayer. In this way, a surface shift of (140 ± 40) meV of the $4f^0$ final state emission was found for β-Ce, which is discussed in connection with f-d hybridization. [S0163-1829(98)03331-1]

I. INTRODUCTION

The electronic structure of Ce-based materials has been subject to numerous experimental[1–9] and theoretical studies,[10–16] in particular in connection with the so-called γ-α phase transition,[17] which is characterized by a volume collapse of $\approx 14\%$ and which is driven by an increase of the hybridization between $4f$ and valence-band states.[6,18] Although studies of weakly hybridized (so-called γ-like) and strongly hybridized (α-like) Ce systems have been performed for several years now, a complete understanding of their $4f$ electronic structure is still lacking. Density functional theory has been successfully used to discuss ground-state properties of Ce systems,[16,19–21] but fails to describe high-energy excitation spectra of these materials. An alternative approach for the description of Ce systems is the Anderson impurity model (AIM),[12,15] which has been successfully applied for a quantitative analysis of spectroscopic data and also allowed a comparison to transport and magnetic properties.[8,15] Its applicability, however, is still a matter of debate, especially in the case of strongly hybridized, α-like Ce systems.[9,19,22–24]

Photoelectron spectroscopy is of particular importance in this discussion, since it allows direct access to the electronic structure. Unfortunately, the interpretation of photoemission (PE) data from Ce systems is not straightforward, since neither a simple one-electron band description nor a pure core-level picture applies in the case of these correlated electronic systems. Moreover, electron spectroscopies are highly surface sensitive, which may aggravate an interpretation in terms of bulk properties. Surface effects on the electronic structure of lanthanide systems are very well known and were extensively studied both for elements[25] and compounds,[26] making particular use of the surface core-level shift (SCS) of the $4f$ states,[27] which can be easily resolved due to the narrow line shapes obtained from these shallow core levels. Closely related to surface energy shifts of the $4f$ states are valence transitions, which lead to an increased $4f$ occupation at the surface.[26] For the heavier lanthanides, this may induce significant changes in the electron spectroscopic data.[28,26]

Surface effects for Ce systems have been first experimentally observed in $3d$ core-level spectroscopy[29] and subsequently also in a more direct way in the $4f$ spectra.[30] In all cases, the surface was found to be characterized by a weaker f-d interaction than in the bulk, leading to a stabilization of a γ-like surface layer on top of a more α-like bulk. This effect has been studied theoretically as well, showing that also on the basis of band-structure slab calculations, a more γ-like character of the surface layer is expected.[20,21]

For Ce metal, such a surface effect was first experimentally observed for the α phase;[30] subsequently, an analogous result was also obtained for γ-Ce.[31] These studies, however, suffered from a presently inevitably low experimental energy resolution, since they made use of $3d \rightarrow 4f$ resonant PE at $h\nu \approx 884$ eV. Furthermore, the studies performed up to now dealt with polycrystalline samples, since clean, well-ordered surfaces were not readily available. With the possibility to grow high-quality films of lanthanide metals on (110) surfaces of bcc metals, however,[32–34] PE studies of well-ordered close-packed lanthanide metal surfaces have become feasible. All these studies showed the necessity of investigating well-characterized surfaces, since the local electronic properties strongly depend on the coordination of the atomic site. For close-packed monocrystalline surfaces, e.g., the SCS's of the heavy lanthanides were found to be systematically smaller than for polycrystalline samples,[32,34,35] suggesting an analogous situation for Ce metal. Furthermore, it was found that all close-packed surfaces of trivalent heavy lanthanide metals exhibit a pronounced surface state with d_{z^2} symmetry around the center of the surface Brillouin zone (BZ), $\bar{\Gamma}$,[34,35]

which is located directly at the Fermi energy E_F, and which is partially occupied. Since the same surface state has also been observed for La metal,[36] it may be expected for a close-packed surface of Ce metal as well, being of particular importance for the f-d interaction.

In this paper we report on a detailed PE study of the electronic structure of a hexagonally ordered film of Ce metal grown at room temperature on W(110). The crystallographic structure of this film is most likely that of the β-Ce phase, which is characterized by similar electronic and magnetic properties as γ-Ce.[17] An important feature of the present work is the investigation of the $4f$ electronic structure of this epitaxial Ce-metal film both in the bulk and at the surface, which could be separated for the first time with the high resolution obtainable at the $4d \rightarrow 4f$ resonance at $h\nu \approx 122$ eV. For an analysis of hybridization and surface effects it is necessary to consider the valence-band structure, which will be discussed in the first part of this paper, where a comparative angle-resolved PE study of the close-packed surfaces of Ce and La is presented in comparison with local-density-approximation (LDA) band-structure calculations. The results are used for an interpretation of the $4f$-PE data obtained at the $4d \rightarrow 4f$ resonance, which will be the topic of the second part. It will be shown by a simple AIM analysis that in analogy to α-Ce, the surface effect in this system is caused by a lowering of the $4f$-level energy and a decrease in f-d hybridization.[30,37]

II. EXPERIMENT

The experiments were performed on well-ordered films of Ce and La metal grown *in situ* on a W(110) substrate. The samples were prepared by deposition of ≈60-Å-thick films, evaporated from resistively heated W coils at rates of ≈5 Å/min, with the substrate held at room temperature. The base pressures in the UHV chambers employed were in the low 10^{-11}-mbar range, rising to $\approx 5 \times 10^{-10}$ mbar during evaporation. Under these conditions, contamination-free films could be grown as monitored by PE at $h\nu = 40$ eV. Subsequent careful annealing to ≈500 K resulted in clean, well-ordered surfaces characterized by sharp hexagonal low-energy electron diffraction (LEED) patterns, confirming that both surfaces are close packed. Further information on the obtained crystal structures was derived from the observed dispersions of band states. As will be discussed below, a comparison with the results of calculations performed for different close-packed crystal structures gives strong evidence that the films grow in a double hcp (dhcp) structure, which is the stable configuration for both metals at temperatures between 150 K and 300 K, used in this experiment. Throughout the paper, the (0001) surfaces refer to such dhcp films.

PE spectra were recorded with two different experimental setups. Angle-resolved PE experiments were performed at the TGM1 beamline of the Berliner Elektronenspeicherring für Synchrotronstrahlung (BESSY) using a VSW-ARIES analyzer with an angular resolution of 2°. The energy resolution ranged from ≈100 meV at $h\nu = 25$ eV to ≈150 meV at higher photon energies. Angle-integrated PE spectra with a resolution of ≈60 meV at $h\nu = 122$ eV were recorded at the high-resolution SX700/II beamline operated by the Freie Universität Berlin at BESSY, using a Leybold EA-11 electron spectrometer. To reduce thermal broadening of the PE lines during the latter experiments, the samples could be cooled with the help of a closed-cycle He refrigerator down to ≈150 K, well above the transition to the α phase of Ce metal.

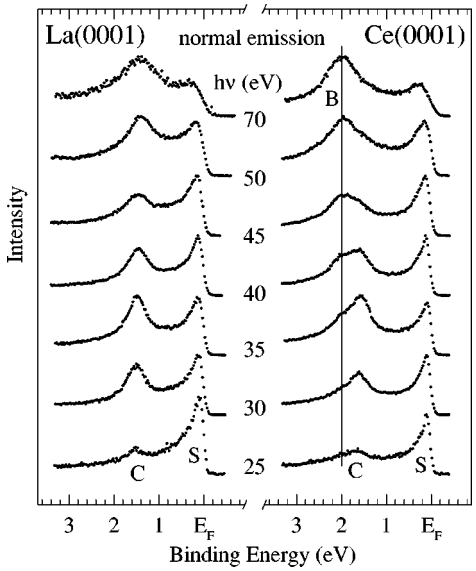

FIG. 1. Angle-resolved photoemission spectra from La(0001) (left) and Ce(0001) (right) recorded at normal emission for various photon energies. Note that the relative spectral intensity from the Ce-$4f^0$ final state increases with increasing photon energy (feature B).

III. VALENCE-BAND STRUCTURE OF Ce(0001) AND La(0001) SURFACES

Band-structure studies with angle-resolved PE have been performed for a number of lanthanide metals.[38–42] While Gd metal—due to its interesting magnetic properties—has been studied most extensively,[40,42,43] only a few studies have been reported for Ce metal.[44,45] In particular, a detailed study of close-packed surfaces of Ce metal has not been performed up to now. In order to elucidate the influence of the $4f$-level occupation on the valence-band structure, a comparative study of Ce and La has been undertaken in the present work.

Figure 1 displays angle-resolved PE spectra of Ce(0001) and La(0001), recorded in normal emission geometry for a number of photon energies between $h\nu = 25$ eV and $h\nu = 70$ eV. For $h\nu = 25$ eV, the cross section of $4f$ PE is rather low;[46] therefore these spectra represent—also in the case of Ce—the pure contribution of valence-band states. The spectra look identical for Ce and La, consisting of two features labeled C and S. Feature C at ≈1.6-eV binding energy (≈1.5 eV in case of La) can be readily identified as due to emission from a bulk band. It disperses only rather weakly with increasing photon energy, in accordance with our band-structure calculations, which show the existence of flat bands along the direction perpendicular to the surface. Feature S is situated in a broad gap of the projected bulk band structure around $\bar{\Gamma}$. For La metal as well as for heavy lanthanide metals, it has been attributed to a localized surface state with d_{z^2} symmetry.[36,47,42] From the right panel of Fig. 1 it is obvious

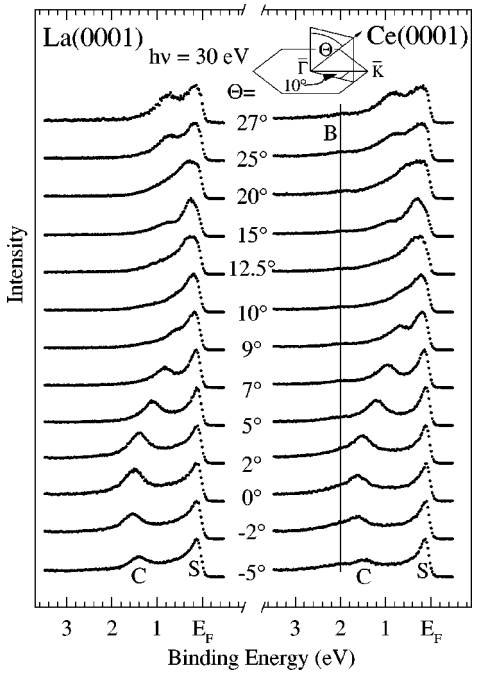

FIG. 2. Angle-resolved photoemission spectra from La(0001) (left) and Ce(0001) (right) recorded at $h\nu=30$ eV for various emission angles Θ. For technical reasons, $k_{\|}$ was not varied along a high-symmetry line of the surface BZ, but with a deviation of 10° relative to $\overline{\Gamma K}$, as indicated by the inset.

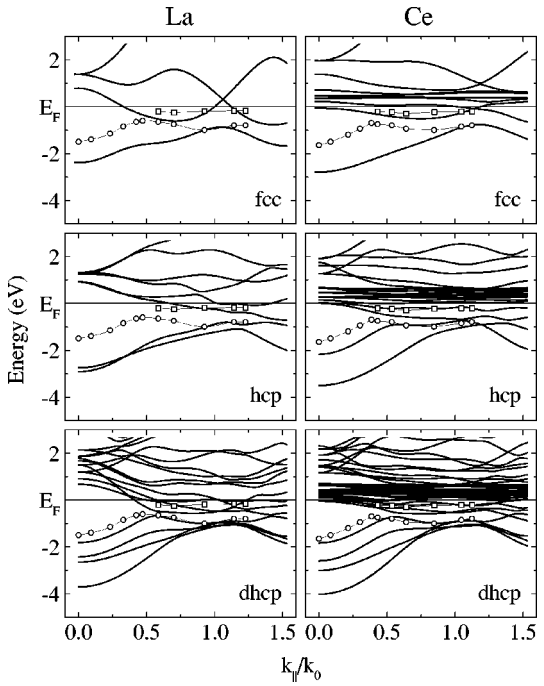

FIG. 3. Band dispersions for La (left) and Ce (right), calculated for three different close-packed crystal structures. The dispersions follow circles in the Brillouin zones (for details, see text). To enable a direct comparison, the $k_{\|}$ values are normalized with respect to the length of $\overline{\Gamma K}$, k_0. The open symbols represent the data of Fig. 2.

that an analogous surface state is also formed at the close-packed surface of Ce metal.

With increasing photon energy, a second feature (B) appears at ≈2-eV binding energy (BE) in the Ce spectra, becoming dominant at the highest photon energy ($h\nu=70$ eV). This behavior reflects a PE final state with mainly $4f^0$ character, since the $4f$ PE cross section increases strongly in the studied photon energy range. Besides this $4f$ structure, which will be discussed in more detail in the next section, and except for the slight differences of the BE of peak C, the spectra of La and Ce are almost identical. This is further confirmed by the angular-dependent PE spectra displayed in Fig. 2. Close similarities of the two systems are found in all details of the band structures: The dispersion of feature C and also the behavior of the surface-state emission S are identical for La and Ce. Feature S does not change over a substantial range of the BZ. Only at larger emission angles does it broaden and additional features appear, which are due to emission from bulk bands. Since a constant photon energy of 30 eV was used in the experiments, the spectra of Fig. 2 reflect the dispersion along a curved line in k space. In Fig. 3, these experimental dispersions are compared to band structures of La and Ce metal calculated along this curve. In addition, calculations were performed for fcc, hcp, and dhcp phases in order to obtain information about the crystal structures of the films.

The calculations were performed in the framework of the local-density approximation with the standard Hedin-Lundquist exchange-correlation potential exploiting the optimized method of linear combination of atomic orbitals[48] (LCAO) in its scalar relativistic version.[49] The basis employed includes $6s$, $6p$, $5d$ atomic valence states for both metals. For Ce, the $4f$ states have been included in the calculations, treating them either as itinerant or alternatively as a localized $4f^1$ configuration. The dispersion of the non-f derived bands was found to be very similar in both cases, with a slightly better agreement with experiment for the itinerant treatment, as displayed in Fig. 3. All phases were handled as ideal crystals without accounting for surface and real structure effects.

For a comparison with the experimental data, direct transitions into free-electron-like final states (parabolic dispersion) and conservation of the component of the electron momentum parallel to the surface were assumed. The minima of the parabolic energy-dispersion curves were pinned to the calculated bottoms of valence bands. The parabolic slopes were fitted to the corresponding s-like branches in the region close to the Γ point by a proper choice of effective electron masses. For constant photon energies, the PE final states are situated approximately on circles in k space, for which the energy dispersions were calculated.[50] The results of these calculations are plotted in Fig. 3 as a function of $k_{\|}$, the component of the wave vector parallel to the surface. The values of $k_{\|}$ are scaled to the respective length of $\overline{\Gamma K}$, k_0, for the different systems, thus allowing a direct comparison. Note that $k_{\|}=0$ does not refer to the center of the BZ, Γ. The calculations show that the main differences between fcc, hcp, and dhcp crystal structures stem from the backfolding of the bands due to the doubling of the respective unit cells. The flat bands seen around the Fermi energy for Ce represent the $4f$ states, treated as itinerant in this case.

The experimentally observed dispersion of feature C in Fig. 2 (open circles in Fig. 3), which is identical for Ce and La except for a small energy offset, is in rather good agreement with the calculations for the dhcp structures. The bands

at higher BE, which have mainly sp character, are not seen in the PE spectra due to small cross sections at the employed photon energies. The comparison of the experimental results with the calculated dispersions for the different phases allows us to draw conclusions about the crystal structure of the epitaxial films. For the fcc phase of Ce, which is stable above room temperature, the position of the bands is not in agreement with the experimental energy position of feature C, which is too close to the Fermi energy. On the basis of the present data, formation of a hcp phase cannot be ruled out, but the agreement is worse than in case of the dhcp phase, which is the thermodynamically stable bulk phase of both La and Ce metal in the used temperature range at low pressures. Therefore the assumption is justified that the epitaxial films studied had dhcp structure.

Projected along the direction perpendicular to the surface, the band structures reveal a broad gap around $\overline{\Gamma}$, a phenomenon characteristic for all close-packed lanthanide-metal surfaces. A similar behavior is also found in slab calculations, which up to now were only performed for Tm, Yb, and Gd.[41,47] In this gap, the localized surface state occurs around $\overline{\Gamma}$, turning into resonances towards the border of the surface BZ, where bulk band states appear. These bulk states are also found in the experimental spectra of Fig. 2 in reasonable agreement with the calculations (open squares in Fig. 3).

These spectroscopic results clearly demonstrate that (i) the valence-band structures of La and Ce are very similar, with negligible influence of the occupied $4f$ states in the latter system and (ii) the close-packed surface of β-Ce metal is characterized by a strongly localized surface state as observed for the other lanthanides. The strong dispersion and the sharpness of the surface-state emission are also an indication of the high crystalline quality of the films.

IV. SURFACE 4f ELECTRONIC STRUCTURE OF β-Ce(0001)

In the past, the surface electronic structure of Ce systems has been examined by different approaches. $3d$ core-level spectroscopy at various photon energies[29] as well as a simultaneous analysis of spectroscopies with varying degrees of surface sensitivity[37] have been applied quite successfully. On the basis of $4f$-PE spectra, a determination of the occupied $4f$ surface electronic structure, however, has only been achieved by the application of resonant PE,[30,31,51,52] exploiting a giant resonant enhancement of the $4f$ photoionization cross section.[7,30] The contribution of the valence states to the resonant spectra has been estimated in the past by considering the off-resonance spectra, where the $4f$ emission is strongly suppressed.[7,30] As discussed further below, this estimate may introduce errors due to a non-negligible resonant enhancement of valence-band emission.[53,54]

A separation of bulk and surface $4f$-PE signals has been achieved by a comparison of resonant PE spectra obtained at the $4d\rightarrow 4f$ resonance ($h\nu\approx 120$ eV) with those obtained at the $3d\rightarrow 4f$ resonance ($h\nu\approx 884$ eV).[30,31,51,52] Due to the high photon energy in the latter case, the surface contribution to the PE spectra is $\approx 20\%$, while it amounts to $\approx 45\%$ at $h\nu\approx 120$ eV.[30] This method, however, has two major disadvantages: At the $3d\rightarrow 4f$ resonance, the energy resolution obtained in a PE experiment up to now is much worse than at the $4d\rightarrow 4f$ resonance, where ≈ 40 meV has been achieved.[30] A separation of bulk and surface contributions is therefore only possible with a loss of information on fine details. Furthermore, the spectral shape of the $4f$ emission changes across the resonance,[7,55,56] aggravating the comparison of data taken at different energies.

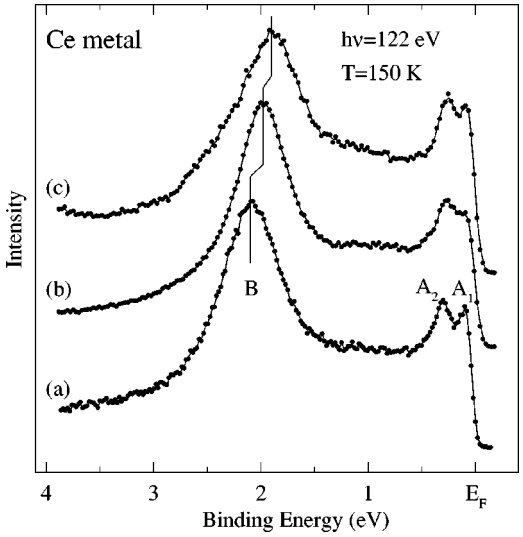

FIG. 4. Photoemission spectra of metallic Ce samples with γ-like f-d hybridization for decreasing degrees of surface roughness, recorded at the $4d\rightarrow 4f$ resonance ($h\nu=122$ eV) in normal emission geometry: (a) scraped bulk sample; (b) epitaxial film. Spectrum (c) was recorded from the same film as (b) after deposition of ≈ 2 monolayers of Dy.

In order to overcome these problems, we have applied a different approach to separate bulk from surface contributions, which cannot be used in the case of rough, polycrystalline surfaces and has only become feasible with the availability of smooth, well-ordered surfaces. In our case, we have suppressed the surface contribution by depositing ≈ 2 monolayers of Dy, which does not contribute to the PE spectra in the energy region of the Ce $4f$ states. For deposition at $T=150$ K, an interdiffusion of the two metals is strongly reduced, and from the similar chemical properties of Dy and Ce neither clustering nor appreciable reactions at the interface are expected. The latter is confirmed by the Dy-$4f$ PE spectra, which do not reveal any chemical shift. With this method, all data could be collected at the $4d\rightarrow 4f$ resonance with an energy resolution high enough to resolve the spin-orbit splitting of the $4f^1$ final state close to E_F. Furthermore, the data were taken at one single photon energy corresponding to the maximum of the $N_{IV,V}$ giant resonance, avoiding in this way artifacts due to differences in the resonant behavior at the $4d\rightarrow 4f$ and $3d\rightarrow 4f$ thresholds, respectively.

The sensitivity of the $4f$ spectrum to changes in the surface order and hence the necessity to investigate well-characterized surfaces is demonstrated in Fig. 4. The PE spectra shown in this figure were taken at the $4d\rightarrow 4f$ resonance at $h\nu=122$ eV from γ-like Ce-metal surfaces prepared by various methods. $4f$-PE spectra of Ce systems reveal three prominent features labeled A_1, A_2, and B. Feature B is predominantly of $4f^0$ character and represents a final state, which is mainly due to emission from a localized $4f^1$ ground state. In a completely unhybridized Ce system, only this fea-

ture is present. A_1 and A_2 result from f-d hybridization and represent a PE final state of mainly $4f^1$ character,[12,14,9] which is supported by the fact that the energy separation of the two peaks corresponds to the atomic spin-orbit splitting.[6] The $4f$ emission close to the Fermi energy is often referred to as the Kondo peak,[8,15] although this assignment is still being lively debated.[22,9] It arises from the interaction of the $4f$ level with the valence band and is most pronounced in α-like Ce systems. In fact, the γ-α phase transition is accompanied by a large increase of the spectral weight at E_F.[6,30] To reduce thermal broadening, the spectra of Fig. 4 were recorded at 150 K, which is necessary to resolve the splitting of A_1 and A_2. This temperature, however, is well above the transition temperature to the α phase.

Spectrum (a) at the bottom of Fig. 4 was recorded from a polycrystalline bulk sample scraped *in situ* with a diamond file, for which the surface is expected to be quite rough.[57] Spectrum (b) was taken from a well-ordered close-packed surface, which was prepared as described in the experimental section and may be assumed to be relatively smooth. It is evident that with decreasing surface roughness, feature B becomes narrower and shifts towards lower BE. This is exactly the behavior expected for a localized, corelike $4f$ state, for which the coordination dependence of the SCS leads to a narrowing and energy shift of the $4f$ emission, if surface and bulk contributions are not experimentally resolved. In addition, changes also take place in the region of features A_1 and A_2. Particularly interesting is the seeming loss of energy resolution in spectrum (b) of the well-ordered film. This, however, is due to the localized surface state, which was shown in the preceding section to be present at the β-Ce(0001) surface and which contributes significantly also at resonance. The surface-state emission is located exactly in the region of A_1 and A_2, filling the dip between the two peaks. This becomes clear if one considers spectrum (c), which was recorded after deposition of ≈ 2 monolayers of Dy metal at 150 K. Here, A_1 and A_2 are clearly separated again, since the surface-state emission has been suppressed. This finding also demonstrates that the contribution of the d states at resonance can be substantial and has to be taken into account in a more careful way than just by considering the off-resonance intensity.[30] After deposition of ≈ 2 monolayers of Dy, the surface emission from Ce can be assumed to be almost completely suppressed. Since in addition the Dy valence-band contributions to the PE spectra are weak as compared to the resonantly enhanced Ce PE, the topmost spectrum of Fig. 4 represents the bulk electronic structure of β-Ce. In the following, we shall describe the procedure to obtain the pure bulk and surface contributions from spectra (b) and (c) of Fig. 4.

As a first step, the background due to inelastically scattered electrons was removed from the two spectra, as well as the weak contribution of the Dy $4f^8$ final-state emission, which occurs as a slight intensity increase around 4-eV BE in spectrum (c). The smooth inelastic background was assumed to be proportional to the area under the PE lines[58,59] and was determined from a fit analysis. The resulting bulk spectrum is shown at the bottom of Fig. 5. In order to obtain the spectral shape for the surface, a properly weighted bulk spectrum was subtracted from spectrum (b) after background removal. For the subtraction, a surface-to-bulk intensity ratio

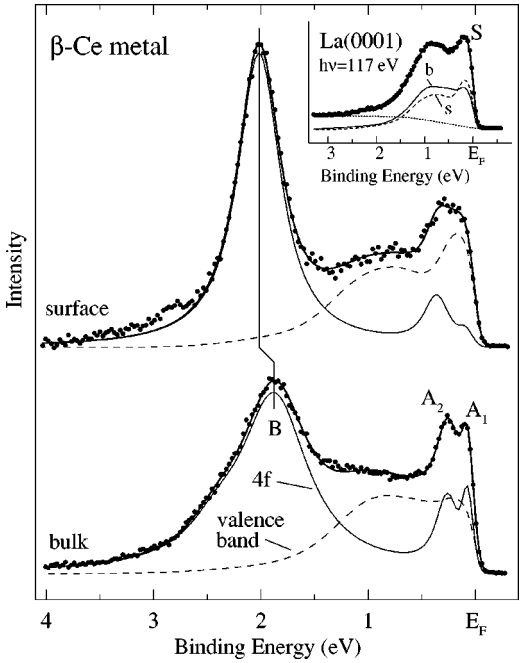

FIG. 5. Bulk and surface resonant PE spectra of β-Ce(0001) obtained from spectra (b) and (c) of Fig. 4 as described in the text, normalized to equal areas. The subspectra represent the result of a fit analysis, which takes the resonant enhancement of valence states into account. The inset shows the resonant PE spectrum from La(0001) together with a decomposition into bulk (solid) and surface (dashed) contributions, which were used for the analysis.

of 0.8 was assumed at $h\nu = 122$ eV, in accordance with experimental data from Sm and Yb metal, where bulk and surface components are readily separated. This number is in fair agreement with calculations of the inelastic mean free path of electrons in this energy range.[30] The resulting spectra, representative of pure bulk and surface contributions, are shown in Fig. 5. Note that they were derived without any assumptions about valence-band contributions at resonance. Two main aspects are clearly visible in these spectra even without any analysis, namely, (i) a shift of feature $B$and (ii) a reduced spectral weight of features A_1 and A_2 at the surface. While the latter has been demonstrated before for a polycrystalline sample, a $4f$-level shift has not been observed for γ-like Ce metal due to insufficient experimental resolution.[30,31] The surface shift amounts to ≈ 140 meV. This is even smaller than expected from the trend of SCS's observed for the close-packed surfaces of other trivalent lanthanide metals,[34,27] from which a value of ≈ 200 meV is estimated. The difference is due to the influence of the f-d hybridization as described in the following.

The influence of the f-d hybridization on the BE of peak B can be understood within the framework of a simple AIM, which considers $4f^0$, $4f^1$, and $4f^2$ configurations and a single valence-band state directly at the Fermi energy.[13,14] Within this model, the spectral function is described by three model parameters, the bare $4f$-level position ϵ_f, the hybridization Δ, and the Coulomb repulsion between two f electrons on the same site, U_{ff}. From these parameters, the spectral weight and the position of feature B can be calculated. If the $4f^2$ configuration is neglected ($U_{ff} \rightarrow \infty$), which is reasonable because for Ce metal $U_{ff} \gg |\epsilon_f|$, Δ, a very simple

formula for the BE of feature B, $\epsilon(B)$, can be derived, which allows us to understand the influence of hybridization in a very easy way:[13]

$$\epsilon(B)=\sqrt{\epsilon_f^2+4\Delta^2}. \quad (1)$$

From this formula it is obvious that a finite hybridization will shift the energy position to a higher BE as compared to the unhybridized case. At the surface of a Ce system, in general, two mechanisms will be important: (i) ϵ_f will lower with respect to E_F, which corresponds to the classical SCS observed for the unhybridized core levels of the heavy lanthanides and (ii) Δ will decrease due to a reduced coordination of the surface atoms. According to Eq. (1), the two effects lead to shifts of opposite directions at the surface. Therefore it could even happen that they cancel each other, leading to a vanishing surface $4f$-level shift. Due to this influence of hybridization, the $4f$-level shift will in general be different from the pure SCS, which is the lowering of ϵ_f at the surface. This is the reason why the identification of a shifted surface component has not been as straightforward for Ce systems as for the heavy lanthanides and always involved spectra measured at different surface sensitivities.[30,31]

In order to be more quantitative in our case, an analysis using the simple AIM was applied to the spectra of Fig. 5.[14] For this purpose, the relative weight and position of feature B had to be determined, which was achieved by applying a fit analysis as shown in Fig. 5. For a quantitative description, it is necessary to account for the d-state contribution in these spectra, which however, is not straightforward. The problem arises from the resonant enhancement of the d-state emission at the $4d\rightarrow 4f$ threshold, which for La metal has been examined in detail recently.[54] Using angle-resolved PE, it was shown that the amount of enhancement of a valence-band feature correlates to the degree of localization of the respective wave function. In Sec. III it was demonstrated that the valence-band structures of La(0001) and Ce(0001) are very similar. Therefore one can expect a resonant enhancement of the d-state cross section also for Ce. In order to estimate the d-band contribution to the resonant spectra of Ce, the intensity increase and the shape of the valence-band emission at the $4d\rightarrow 4f$ resonance of La was measured for La(0001) in the same experimental setup. The inset of Fig. 5 displays a resonant PE spectrum of La, which consists of emission from the bulk bands (D) and also from the surface state (S). It was found that the spectral intensity increases by a factor of ≈ 7 at resonance. Unfortunately, a simple transfer of that number to the Ce case is not possible, since the resonant behavior cannot be expected to be identical for La and Ce. This is due to the different occupation of the $4f$ states in Ce, which opens different excitation and decay channels at the $4d\rightarrow 4f$ resonance. A quantitative description of these influences is beyond the scope of this paper. One can expect, however, that due to the opening of the important decay channel of $4f$ emission, the resonance of the d states will be weaker in Ce than in La.

With this proviso, the spectra of Fig. 5 were fitted using three Lorentzian line shapes for the $4f$ emission, A_1, A_2, and B, cut at E_F by a Fermi-Dirac function. In the case of the bulk spectrum, an additional line was used to account for the asymmetry of feature B. The shapes of the valence-band contributions to the bulk and surface spectra were estimated from the bulk and surface spectra of La metal derived in an analogous way as for Ce by quenching with Dy. The inset displays a resonant PE spectrum of La metal, together with a decomposition into bulk (b, solid) and surface (s, dashed) contributions. The intensities of the respective valence-band contributions were scaled to fit the Ce spectra at $\approx$1-eV BE. This resulted in a valence-band spectral weight of $\approx$35%, which is in fact less than what one would expect, if the resonance behavior in La and Ce was identical. In this way, a reasonable fit was achieved for the bulk and the surface spectrum, as given by the solid line through the data points. The solid and dashed subspectra represent the pure $4f$ emission and the valence-band contribution, respectively. From the position of feature B and its relative weight with respect to A_1 and A_2, the AIM parameters ϵ_f, Δ, as well as the f occupation number n_f were calculated for the bulk and the surface, assuming $U_{ff}=6$ eV.[14] The exact value of this latter parameter is not crucial, since it is anyway large compared to the other two. The values found for the bulk are $\epsilon_f^b=-1.6$ eV, $\Delta^b=0.4$ eV, while for the surface $\epsilon_f^s=-1.8$ eV, $\Delta^s=0.3$ eV were derived. The corresponding $4f$ occupancies are $n_f^b=0.96$ and $n_f^s=0.98$. This analysis shows that the surface effect in β-Ce is indeed caused by the two effects mentioned above: The bare $4f$-level energy is lowered, with the shift of 0.2 eV being in full agreement with the trend observed for other close-packed lanthanide surfaces.[34] The relative decrease of the hybridization is comparable to the case of polycrystalline α-Ce,[30,37] and reflects the effect of the reduced coordination at the surface. The observed decrease of Δ might be somehow surprising, considering the presence of the d-like surface state and its large density of states at E_F, $D(E_F)$. Since the hybridization is proportional to $D(E)$,[37] with the states at E_F being of particular importance, even an increase at the surface could be expected, despite the reduced number of neighbor atoms. This seeming discrepancy, however, can be explained by the strongly localized, atomiclike character of the surface state, which for symmetry reasons may lead to a vanishing on-site hybridization with the f states.[12] The absolute values, especially of the hybridization parameters, should not be overinterpreted, since the AIM analysis applied here does not take the valence-band structure properly into account. Furthermore, the thermal dependence of features A_1 and A_2 as described by the noncrossing approximation has not been considered here.[8,9] Therefore the values of Δ, which were obtained from spectra recorded at finite temperature, are supposed to underestimate the f-d hybridization. Nevertheless, the above comparison of bulk and surface parameters is meaningful, since it refers to analyses within the same AIM model using spectra recorded at the same temperature.

A quantitative analysis of bulk and surface parameters for γ-Ce has been performed by Liu *et al.*,[37] which takes the valence-band structure detailed into account, and which leads to quite similar results. The $4f$ occupancies, e.g., are very similar to the present values, close to $n_f=1$. The hybridization parameters of that study are not simply comparable to the present values, since they were derived taking the whole band structure into account. They exhibit, however, a similar behavior, namely, a decrease at the surface.

The $4f$-level positions, however, are quite different from the present results, leading to a SCS of 0.46 eV, which is much larger than the value of 0.2 eV derived here. This is probably due to the fact that monocrystalline samples were studied here, whereas the former result refers to polycrystalline surfaces, where in fact a larger SCS is expected (Fig. 4).

Finally, we would like to comment on the feasibility of an analogous experiment for a monocrystalline film of α-Ce metal. All attempts to prepare such films have failed, since they had to be grown at temperatures as low as 40 K in order to ensure an α-like character as determined by resonant $4f$ PE.[30] These films were characterized by PE spectra similar to those obtained from films deposited on polycrystalline substrates[30] and showed no LEED pattern. Upon careful stepwise annealing to increase the film order, the $4f$ spectra became more and more γ-like. After eventually achieving a well-ordered surface with a reasonable LEED pattern, the films showed PE spectra like the one presented in Fig. 4(b), i.e., the films were no longer α-like.

V. CONCLUSIONS

In this contribution we have presented a detailed PE study of the surface electronic structure of β-Ce(0001). The valence-band structure of this material, as revealed by angle-resolved PE, was found to be almost identical to that of La(0001), despite the additional $4f$ electron in Ce. The observed dispersions were found to agree well with standard LDA band-structure calculations. It was shown that the localized surface state at E_F, which is characteristic for all close-packed lanthanide-metal surfaces, is also present in β-Ce. For a correct determination of the surface $4f$ electronic structure in Ce systems, well-ordered surfaces were found to be crucial, as in the case of the heavy lanthanides, in particular concerning BE shifts of the $4f^0$ final-state feature. By quenching the surface emission with a thin Dy overlayer, it was possible to separate bulk and surface contributions in high-resolution resonant PE at the $4d \rightarrow 4f$ threshold. From the data, a surface shift of the $4f^0$ component of 140 ± 40 meV was obtained, which is in full agreement with SCS's of the heavy lanthanide metals if hybridization effects are properly taken into account.

ACKNOWLEDGMENTS

The work in Berlin was supported by the Bundesminister für Bildung, Wissenschaft, Forschung und Technologie, Project No. 05-625 KEC, and by the Deutsche Forschungsgemeinschaft Sfb-290/TPA06. The work in Dresden was supported by the Bundesminister für Bildung, Wissenschaft, Forschung und Technologie, Project No. 05-625 ODA, and by the Deutsche Forschungsgemeinschaft Sfb-468/TPB04.

*On leave from Institute of Physics, St. Petersburg State University, 198904 St. Petersburg, Russia.

†Permanent address: Institut für Theoretische Physik, Technische Universität Dresden, D-01062 Dresden, Germany.

[1] R. D. Parks, N. Mårtensson, and B. Reihl, in *Valence Instabilities*, edited by P. Wachter and H. Boppart (North-Holland, Amsterdam, 1982), p. 239.

[2] J. C. Fuggle, F. U. Hillebrecht, J.-M. Esteva, R. C. Karnatak, O. Gunnarsson, and K. Schönhammer, Phys. Rev. B **27**, 4637 (1983).

[3] E. Wuilloud, H. R. Moser, W.-D. Schneider, and Y. Baer, Phys. Rev. B **28**, 7354 (1983).

[4] D. M. Wieliczka, C. G. Olson, and D. W. Lynch, Phys. Rev. B **29**, 3028 (1984).

[5] E. Jensen and D. M. Wieliczka, Phys. Rev. B **30**, 7340 (1984).

[6] F. Patthey, B. Delley, W.-D. Schneider, and Y. Baer, Phys. Rev. Lett. **55**, 1518 (1985).

[7] J. W. Allen, S.-J. Oh, O. Gunnarsson, K. Schönhammer, M. B. Maple, M. S. Torikachvili, and I. Lindau, Adv. Phys. **35**, 275 (1986).

[8] F. Patthey, J. M. Imer, W.-D. Schneider, H. Beck, Y. Baer, and B. Delley, Phys. Rev. B **42**, 8864 (1990).

[9] D. Malterre, M. Grioni, and Y. Baer, Adv. Phys. **45**, 299 (1996).

[10] J. W. Allen and R. M. Martin, Phys. Rev. Lett. **49**, 1106 (1982).

[11] R. Podloucky and D. Glötzel, Phys. Rev. B **27**, 3390 (1983).

[12] O. Gunnarsson and K. Schönhammer, Phys. Rev. Lett. **50**, 604 (1983); Phys. Rev. B **28**, 4315 (1983).

[13] A. Fujimori, Phys. Rev. B **28**, 4489 (1983).

[14] J. M. Imer and E. Wuilloud, Z. Phys. B **66**, 153 (1987).

[15] N. E. Bickers, D. L. Cox, and J. W. Wilkins, Phys. Rev. B **36**, 2036 (1987).

[16] Z. Szotek, W. M. Temmerman, and H. Winter, Phys. Rev. Lett. **72**, 1244 (1994); A. Svane, *ibid.* **72**, 1248 (1994).

[17] D. C. Koskenmaki and K. A. Geschneidner, Jr., in *Handbook on the Physics and Chemistry of the Rare Earths*, edited by K. A. Geschneidner, Jr. and L. R. Eyring (North-Holland, Amsterdam, 1978), Vol. 1.

[18] C. Gu, X. Wu, C. G. Olson, and D. W. Lynch, Phys. Rev. Lett. **67**, 1622 (1991).

[19] E. Weschke, C. Laubschat, R. Ecker, A. Höhr, M. Domke, G. Kaindl, L. Severin, and B. Johansson, Phys. Rev. Lett. **69**, 1792 (1992).

[20] O. Eriksson, R. C. Albers, A. M. Boring, G. W. Fernando, Y. G. Hao, and B. R. Cooper, Phys. Rev. B **43**, 3137 (1991).

[21] O. Eriksson, J. Trygg, O. Hjortstam, B. Johansson, and J. M. Wills, Surf. Sci. **382**, 93 (1997).

[22] J. J. Joyce, A. J. Arko, J. Lawrence, P. C. Canfield, Z. Fisk, R. J. Bartlett, and J. D. Thompson, Phys. Rev. Lett. **68**, 236 (1992).

[23] S. Hüfner, Z. Phys. B **86**, 241 (1992).

[24] M. Garnier, K. Breuer, D. Purdie, M. Hengsberger, Y. Baer, and B. Delley, Phys. Rev. Lett. **78**, 4127 (1997).

[25] F. Gerken, A. S. Flodström, J. Barth, L. I. Johansson, and C. Kunz, Phys. Scr. **32**, 43 (1985).

[26] C. Laubschat, G. Kaindl, W.-D. Schneider, B. Reihl, and N. Mårtensson, Phys. Rev. B **33**, 6675 (1986).

[27] M. Aldén, B. Johansson, and H. L. Skriver, Phys. Rev. B **51**, 5386 (1995).

[28] G. K. Wertheim and G. Crecelius, Phys. Rev. Lett. **40**, 813 (1978).

[29] C. Laubschat, E. Weschke, C. Holtz, M. Domke, O. Strebel, and G. Kaindl, Phys. Rev. Lett. **65**, 1639 (1990).

[30] E. Weschke, C. Laubschat, T. Simmons, M. Domke, O. Strebel, and G. Kaindl, Phys. Rev. B **44**, 8304 (1991).

[31] L. Duò, S. De Rossi, P. Vavassori, F. Ciccacci, G. L. Olcese, G.

Chiaia, and I. Lindau, Phys. Rev. B **54**, R17 363 (1996).
[32] E. Navas, K. Starke, C. Laubschat, E. Weschke, and G. Kaindl, Phys. Rev. B **48**, 14 753 (1993).
[33] B. Kierren, T. Gourieux, F. Bertran, and G. Krill, Phys. Rev. B **49**, 1976 (1994).
[34] G. Kaindl, A. Höhr, E. Weschke, S. Vandré, C. Schüßler-Langeheine, and C. Laubschat, Phys. Rev. B **51**, 7920 (1995).
[35] E. Weschke and G. Kaindl, J. Electron Spectrosc. Relat. Phenom. **75**, 233 (1995).
[36] A. V. Fedorov, A. Höhr, E. Weschke, K. Starke, V. K. Adamchuk, and G. Kaindl, Phys. Rev. B **49**, 5117 (1994).
[37] L. Z. Liu, J. W. Allen, O. Gunnarsson, N. E. Christensen, and O. K. Andersen, Phys. Rev. B **45**, 8934 (1992).
[38] D. Li, C. W. Hutchins, P. A. Dowben, C. Hwang, R.-T. Wu, M. Onellion, A. B. Andrews, and J. L. Erskine, J. Magn. Magn. Mater. **99**, 85 (1991).
[39] S. C. Wu, H. Li, Y. S. Li, D. Tian, J. Quinn, F. Jona, and D. Fort, Phys. Rev. B **44**, 13 720 (1991).
[40] B. Kim, A. B. Andrews, J. L. Erskine, K. J. Kim, and B. N. Harmon, Phys. Rev. Lett. **68**, 1931 (1992).
[41] M. Bodenbach, A. Höhr, C. Laubschat, G. Kaindl, and M. Methfessel, Phys. Rev. B **50**, 14 446 (1994).
[42] P. A. Dowben, D. N. McIlroy, and D. Li, in *Handbook on the Physics and Chemistry of the Rare Earths*, edited by K. A. Geschneidner, Jr. and L. R. Eyring (North-Holland, Amsterdam, 1996), Vol. 24.
[43] E. Weschke, C. Schüßler-Langeheine, R. Meier, A. V. Fedorov, K. Starke, F. Hübinger, and G. Kaindl, Phys. Rev. Lett. **77**, 3415 (1996).
[44] G. Rosina, E. Bertel, F. P. Netzer, and J. Redinger, Phys. Rev. B **33**, 2364 (1986).
[45] E. Vescovo and C. Carbone, Phys. Rev. B **53**, 4142 (1996).
[46] J. J. Yeh and I. Lindau, At. Data Nucl. Data Tables **32**, 1 (1985).
[47] R. Wu, C. Li, A. J. Freeman, and C. L. Fu, Phys. Rev. B **44**, 9400 (1991).
[48] H. Eschrig, *Optimized LCAO Method* (Springer, Berlin, 1989).
[49] M. Richter and H. Eschrig, Solid State Commun. **53**, 529 (1989).
[50] N. V. Smith and L. F. Mattheiss, Phys. Rev. B **9**, 1341 (1974).
[51] C. Laubschat, E. Weschke, M. Domke, C. T. Simmons, and G. Kaindl, Surf. Sci. **269/270**, 605 (1992).
[52] G. Chiaia, P. Vavassori, L. Duò, L. Braicovich, M. Quarford, and I. Lindau, Surf. Sci. **331–333**, 1229 (1995).
[53] C. G. Olson, P. J. Benning, Michael Schmidt, D. W. Lynch, P. Canfield, and D. M. Wieliczka, Phys. Rev. Lett. **76**, 4265 (1996).
[54] S. L. Molodtsov, M. Richter, S. Danzenbächer, S. Wieling, L. Steinbeck, and C. Laubschat, Phys. Rev. Lett. **78**, 142 (1997).
[55] O. Gunnarsson and T. C. Li, Phys. Rev. B **36**, 9488 (1987).
[56] C. L. Nicklin, C. Binns, S. Mozley, C. Norris, E. Alleno, M.-G. Barthés-Labrousse, and G. van der Laan, Phys. Rev. B **52**, 4815 (1995).
[57] W.-D. Schneider, C. Laubschat, and B. Reihl, Phys. Rev. B **27**, 6538 (1983).
[58] H. Höchst, P. Steiner, G. Reiter, and S. Hüfner, Z. Phys. B **42**, 199 (1981).
[59] G. K. Wertheim and S. B. DiCenzo, J. Electron Spectrosc. Relat. Phenom. **37**, 57 (1985).